Temperature Dependent Electrical Properties of Combustion Synthesized $GdAlO_3$ Perovskite

Saji S K[1], Jeyasingh T [1], Vinodkumar R[1], P R S Wariar[1] and Radhakrishnan [2,a)]

[1]*Department of Physics,University College, Thiruvananthapuram, Kerala-695034 (India)*
[2]*Department of Theoretical Physics, University of Madras, Chennai- 600025 (India).*
[a)]*Corresponding author. E-mail address: rkrishna.tp@gmail.com*

Abstract: Gadolinium aluminate ($GdAlO_3$) perovskite has been prepared from Gadolinium oxide and Aluminium nitrate by auto-igniting combustion process. HR-SEM image of sintered pellet of the sample suggest polycrystalline microstructure with the grains of unequal size distributed throughout the sample. Temperature and frequency dependence of electrical properties have been investigated for the sample in the frequency range 1Hz-1MHz. The dielectric characteristics of the sample have been studied by analyzing electric conductivity, dielectric spectra, dielectric loss and electric modulus formalism. The frequency dependent ac conductivity has been analyzed by using Jonscher's universal power law. The frequency exponent (n) have been found to be temperature dependent. The behavior of n with increase in temperature further suggested that the ac conduction mechanism of the studied samples follows the overlapping large polaron tunneling (OLPT) model.

Key words: perovskite, dielectric spectra, modulus formalism, ac conductivity.

INTRODUCTION

Rare earth aluminates ($RAlO_3$) perovskite have great interest in material science due to their many diverse electric, magnetic, optical, and catalytic properties, apart from the academic point of view due to physical properties they exhibits [1]. Investigations on the microwave dielectric properties of rare earth aluminates revealed that most of them have suitable permittivity and quality factor but with modification of tau (f) could be used for dielectric resonator applications. Size of dielectric resonators and transmission–line substrates depends greatly on the value of dielectric constant as it is proportional to $1/\sqrt{\varepsilon_r}$. Rare earth aluminates (Ln= Dy, Er, La, Nd, Pr, Sm, Y) have high permittivity in microwave region, make them suitable materials for miniaturization of such devices [2]. Also, RAlO3 perovskite have very low dielectric loss and have been used as a substrate material for YBCO superconductor [3].

Gadolinium aluminates (GdAlO3) is a technologically important RAlO3-type perovskite oxide which have applications as phosphor , scintillator , as well as a potential host system for materials with oxygen ion conductivity [4,5]. The objective of this study is to investigate electric transport properties of $GdAlO_3$orthoaluminate by employing dielectric spectroscopy, electric modulus formalism and conductivity studies over a wide range of frequencies and temperatures, which can give fundamental information on the mechanism of electric conduction and relaxation process.

EXPERIMENTAL TECHNIQUE

Samples were prepared using combustion synthesis. The starting materials used in the synthesis of the sample were stochiomertic amount of high purity (99.99%, Sigma Aldrich) Gd_2O_3 and $Al(NO)_3.9H_2O$. Gd_2O_3 was dissolved in concentrated nitric acid and $Al(NO)_3.9H_2O$ in distilled water and they were mixed to form an aqueous solution. Proper amount of citric acid was added into the solution to maintain anion to cation ratio at unity. The oxidant fuel ratio of the system was adjusted using nitric acid and ammonium hydroxide. The solution containing the complex precursor at neutral pH was heated on a hot plate to about 250^0C. The solution boiled on heating, underwent dehydration and decomposition leading to a smooth deflation, producing foam and self-ignited on persistent heating resulting in a fluffy and voluminous combustion powder.

The combustion powder after calcinated at 1000^0C for 2 h was examined by x-ray diffraction (XRD). XRD (Mac Science, Model MPX18, Japan) data were collected using Cu K_α radiation and a graphite monochromator with a 2(theta) range from 10^0 to 90^0. A step scan with a step size of 0.02 was used with counting time of 1 s /step. The powder was pressed uniaxially into cylindrical pellets at a pressure of 100 MPa by using a hydraulic press. The specimen was sintered at 1400^0C for 4 hrs in air. Bulk density of the sintered specimen was measured using Archimedes method. The sintered specimen attained a relative density 97% of theoretical density of the material. Dielectric properties of sintered specimens were measured as a function of frequency (1Hz-1MHz) at various temperatures by using NOVO-CONTROL (Alpha-A) high-performance frequency analyzer.

RESULTS AND DISCUSSION

Structure and Morphology

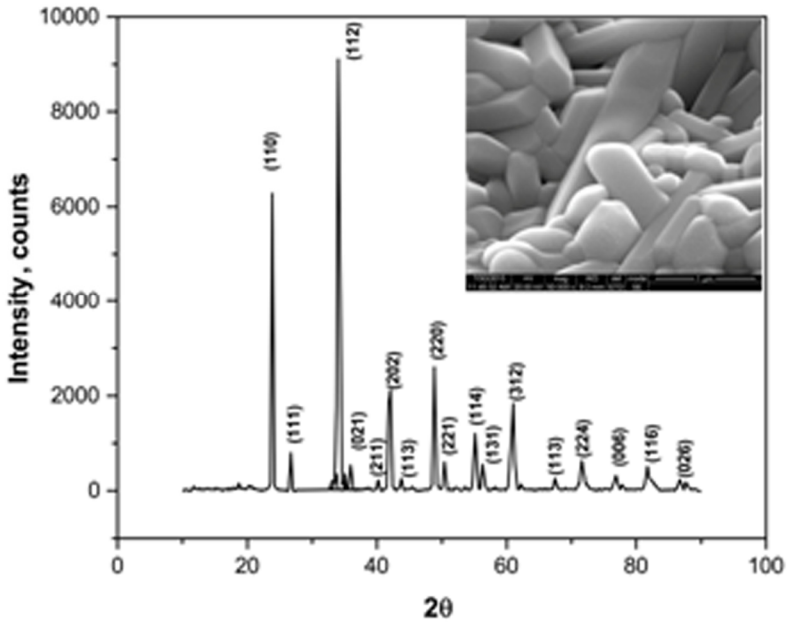

Fig. 1 XRD pattern of $GdAlO_3$ sample calcinated at 1000^0 C for 2 h (inset shows HR-SEM image of sintered pellet)

Fig 1. Shows the XRD pattern of the sintered $GdAlO_3$ sample that matched with the orthorhombic perovskite structure. All the peaks in the XRD pattern are in good agreement with ICDD card No.46−0395,

demonstrating the formation of $GdAlO_3$ phase with orthorhombic perovskite structure. Lattice parameters calculated from the diffraction pattern where a = 5.2604 Å, b = 5.2065 Å, and c = 7.3547 Å, which match very well with the reported values [6]. No diffraction peak that could be related to impurity or secondary phase was observed in the XRD pattern. The average size of the crystallites calculated from the XRD peaks following the Scherrer formula was ~39nm. The optimum sintering temperature was determined by sintering the compacted specimens at different temperatures in the range 1200–1600^{0}C for duration of 4 h. The maximal density was obtained at 1400^{0}C for 4 h which is chosen as the optimal sintering temperature for $GdAlO_3$. The high densification is achieved without using any sintering aids.

The microstructural of the sample is characterized by high resolution scanning electron microscopy. Inset of Fig. 1 shows HR-SEM of $GdAlO_3$ sample sintered at 1400^{0}C for 4h. The HR-SEM image shows well crystallized sub-micron lode like grains with sharp grain boundaries. It is clear from the micrograph that densification was achieved without significant microstructural coarsening.

AC Conductivity Analysis

Measurement of frequency dependent ac conductivity is a useful technique to characterize the electric transport process in ceramic perovskite. The electrical conduction in perovskite oxides results from thermal activation of electrons from in the ionic lattice. Fig. 3(a) depicts frequency dependence of ac conductivity at various temperatures for the prepared $GdAlO_3$ ceramics. The plots show that the ac conductivity almost remains constant at low frequencies but exhibit dispersion for higher frequencies.

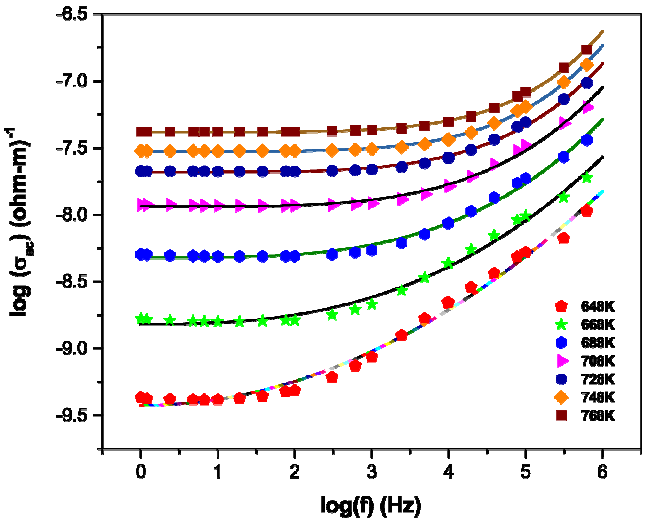

Fig. 2 Frequency dependency of electrical conductivity at different temperatures. Solid lines are the theoretical fit.

The ac conductivity behavior is analyzed using conductivity formalism, i.e. Jonscher's universal power law [7]:

$$\sigma_{ac} = \sigma_{dc} + A\omega^n \qquad (1)$$

where σ_{ac} represents the ac conductivity, σ_{dc} is the dc conductivity at given temperature, A is the temperature dependent parameter, n is the power law exponent and ω is the angular frequency of applied ac field.

The exponent n represents the degree of interaction between the mobile ions with the lattice and theoretically has the value between 0 and 1 depending upon temperature. The typical value of n lies between 0 and 1, ac conduction

is through hopping mechanism. The n value is determined from the slope of linear part of σ_{ac} versus ω curve. The presently studied ceramic samples have been found to obey the Jonscher's universal power law at all the temperatures and frequencies.

The observed frequency dependent conductivity behavior can be related to the bound carriers trapped in the energy levels of the localized sites. The frequency dependence of the ac conductivity at higher frequency and at various temperatures resembles that of hopping-type conduction between these trap centers. Further, the rise in the value of conductivity with temperature indicates that electrical conductivity in the material is a thermally activated process. The activation energy for the dc conductivity is obtained by using the Arrhenius relation:

$$\sigma_{dc}\, T = \sigma_0 \exp\left(-\frac{E_{dc}}{kT}\right) \tag{2}$$

where σ_0 is pre-exponential dc conductivity E_{dc} is the activation energy for dc conduction. The activation energy (E_{dc}) for the dc conduction has been calculated from the slope of $\ln(\sigma_{dc})$ vs $(1000/T)$ (Fig. 3(a)) and its value is found to be 0.76 eV. This value of activation energy determined from the Arrhenius plot suggests that conduction may be due to hopping of charge carriers.

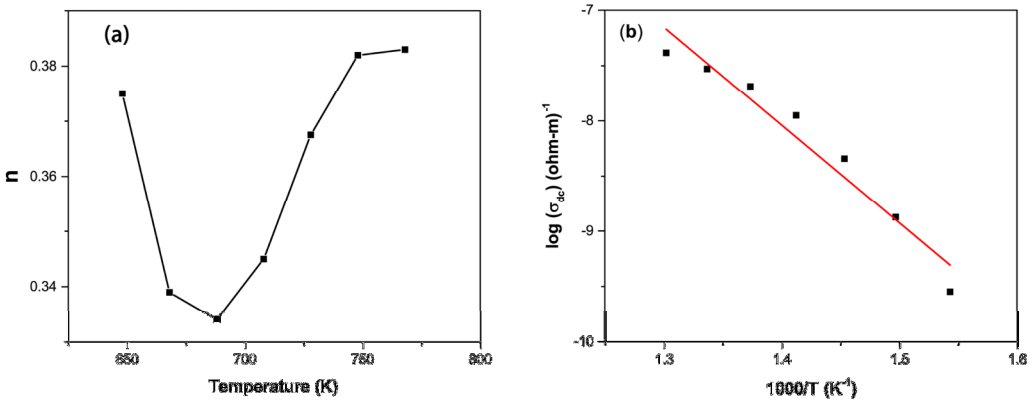

Fig. 3(a) Variation of frequency exponent n with temperature and (b) Arrhenius plot for dc conductivity

The frequency dependent hopping conduction is further analyzed based on the variation of n as a function of temperature. Four different models based on classical hopping of a carrier over the potential barrier separating two energetically favorable sites and quantum-mechanical tunneling through the barrier separating two equilibrium positions, were proposed to investigate the conduction mechanism [8,9];

i. Quantum mechanical tunneling (QMT), if n depends upon frequency but independent of temperature.
ii. Small polaron hopping (SPH) conduction, when n increases with temperature.
iii. Correlated barrier hopping (CBH), when n decreases with increase in temperature.
iv. Overlapping large polaron tunneling (OLPT), if the n value first decreases and then increases with increase in temperature .

The value of n can be obtained from the slopes of the plots $\log(\omega)$ vs $\log(\sigma_{ac})$ and 'A' from the intercept. The ac conductivity spectra for different temperatures were fitted with equation (1). Fig. 3(a) depicts behavior of n obtained for the ceramic sample under study and is consistent with that of the OLPT model, suggesting that the conduction mechanism in these ceramics could be analyzed using overlapping large polaron tunneling (OLPT).

Dielectric Properties

The frequency dependence of the dielectric constant (ε') and loss tangent (tan δ) at various temperatures for the synthesized $GdAlO_3$ sample has been studied. Fig. 4(a) and 4(b) respectively depict log (f) vs ε′ and log (f) vs log $tan\ \delta$ plots at different temperatures. It is observed that at low frequencies, the dispersion of dielectric constant and $tan\ \delta$ is observed for all the temperatures. As the temperature rises there is an abrupt increase in the dielectric constant and dielectric loss tangent. However, this increase is more prominent in the low frequency region.

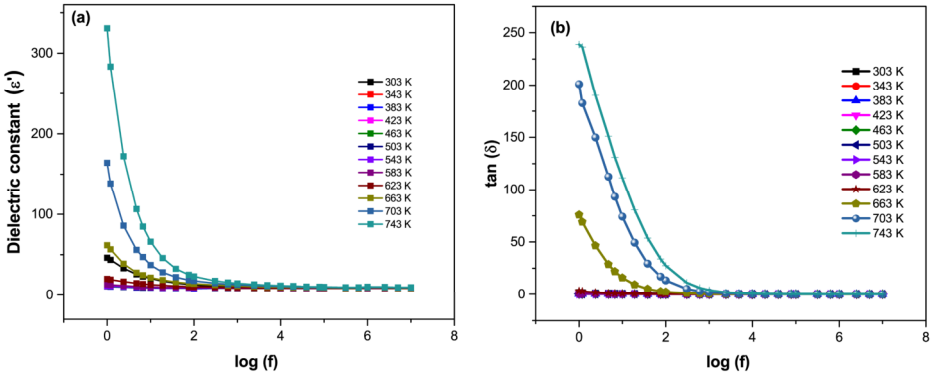

Fig. 3(a) Variation of real part of dielectric constant ε′ and (b) loss tangent tanδ with frequency and temperatures for $GdAlO_3$

At the higher frequency region ε' and tanδ decreases gradually and attain a constant limiting value. The strong dispersion in the low frequency region and the high value of the measured dielectric constant is caused by the total polarization resulting from the orientation of the dipole and trapped charge carriers [10]. Dielectric loss is the electrical energy lost as heat in the polarization process in the presence of an applied ac field. The high values of ε′ interestingly observed only at very high temperature and very low frequencies may be attributed to the fact that the free charges buildup at interfaces within the bulk of the sample and at the interface between the sample and the electrodes space charge polarization [11].

Electric modulus formalism

The complex electric modulus is the reciprocal of complex permittivity, i.e. $M^* = 1/\varepsilon^*$. Modulus formalism is now widely used to analyze relaxation properties of ionic conductors and polycrystalline ceramics. Advantage of complex electric modulus formalism is that it can easily distinguish electrode polarization effect from grain boundary conduction process. The electric modulus corresponds to the relaxation of electric field in the material when the electric displacement remains constant, so that the electric modulus represents the real dielectric relaxation process. Hence it is useful in detecting bulk properties as apparent conductivity relaxation times. Generally for a pure ionic conduction process, a relaxation peak would be appear in the frequency spectra of imaginary component M'' and no peak would appear in the corresponding plot of ε''. However for a dielectric relaxation process, a relaxation peak would appear in both M^* and ε^* representations. The complex electric modulus $M^*(\omega)$ is expressed as,

$$M^*(\omega) = 1/\varepsilon^*(\omega) = \frac{\varepsilon'}{(\varepsilon')^2+(\varepsilon'')^2} + \frac{\varepsilon''}{(\varepsilon')^2+(\varepsilon'')^2} = M' + iM'' \quad (3)$$

where ε', ε'',$M'$and M'' are real component of permittivity, imaginary component of permittivity, real component of electric modulus and imaginary component of electric modulus respectively.

The frequency dependence of electric modulus of the synthesized $GdAlO_3$ ceramic was studied in the temperature range from 303 K to 743 K and frequency range from 1 Hz to 1 MHz. The obtained modulus spectra

$M'(\omega)$ and $M''(\omega)$ are depicted figures 5(a) and 5(b). It is observed that at low frequencies M' approaches zero for all the given temperatures. This is due to lack of restoring forces for the mobile ions present in the material. In the high frequency region M' increases continuously and approaches a maximum value which corresponds to $M_\infty = (\varepsilon_\infty)^{-1}$ due to relaxation phenomenon. The maximum value of M' decreases with increase in temperature indicates that the conduction process in the material is due to the short range mobility of charge carriers. M'' spectra exhibit a pronounced relaxation peak that move towards higher frequency side with increasing temperature. These peaks indicate the transition from long range to short range mobility with increasing frequency. The low frequency side of the peak represents the range of frequencies in which the ions are capable of moving long distances, i.e. performing successful hopping from one site to neighboring site, whereas, for the high frequency side, the ions are spatially confined to their potential wells and can execute only localized motion. The shifting of the peak position towards the higher frequency region with increasing temperature indicates thermally activated nature of relaxation time.

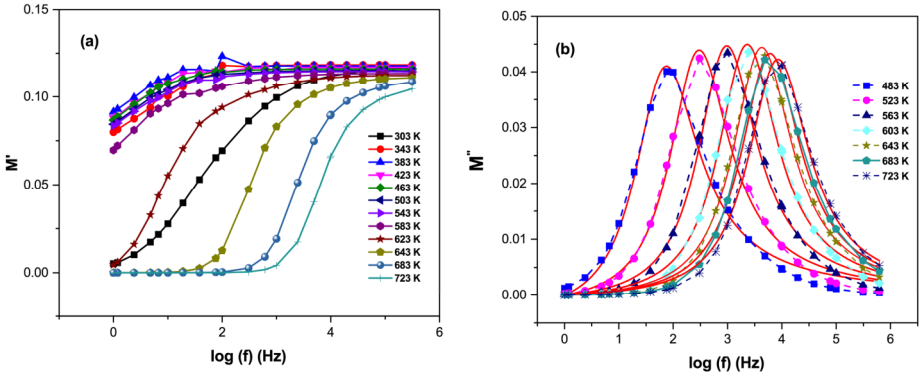

Fig. 4(a) Real and (b) imaginary parts of electric modulus spectra at different temperatures. Solid lines are the theoretical fit.

The electric field relaxation due to motions of charge carriers is generally well described by the empirical Kohlrausch–Williams–Watts (KWW) function. This function represents the distribution of relaxation time in non-conducting materials [12]:

$$\phi(t) = \exp\left[-\left(\frac{t}{\tau_m}\right)^{\beta}\right] \tag{4}$$

where the exponent β indicate deviation from Debye type relaxation and τ_m is the conductivity relaxation time. The smaller the value of β, the larger the deviation of the relaxation with respect to a Debye-type relaxation (β=1). M^* may be expressed as Fourier transform of relaxation function $\phi(t)$.

$$M^*(\omega) = M_\infty\left[1 - \int_0^\infty \left(-\frac{d\phi}{dt}\right)\exp(-i\omega t)dt\right], \tag{5}$$

where $M_\infty = (\varepsilon_\infty)^{-1}$ is the asymptotic value of $M'(\omega)$.

In the present study modified KWW function introduced by Bergman [13] has been used to rationalize the electric modulus behavior of $GdAlO_3$ ceramic samples. In this function, the imaginary part of electric modulus may be expressed as

$$M'' = \frac{M''_{max}}{(1-\beta)+\frac{\beta}{1+\beta}\left[\beta\left(\frac{f_{max}}{f}\right)+\left(\frac{f}{f_{max}}\right)^{\beta}\right]} \tag{6}$$

where M''_{max} is the maximum value of M'' and f_{max} is the corresponding frequency. The Fig. 6(b) depicts theoretical fit of the above equation with the experimental data of M''. From the figure, it is clearly seen that the

experimental data is well fitted to this model. Value of β obtained by fitting the frequency plot of M″is observed to be less than 1, suggesting that the relaxation process in the presently studied system is non-Debye type. Also, the values of β have been found to increase with increase in temperature.

Conclusion

Electric transport properties of Gadolinium monoaluminate ($GdAlO_3$) were investigated. The frequency dependent electrical data were analyzed in the frame work of conductivity, dielectric spectroscopy and electric modulus formalism over a wide range temperature under different frequency range (1Hz-1MHz). The observed dispersion behavior of ac conductivity of the studied sample has been found to obey Jonscher's universal power law. The temperature dependence of the exponent n was investigated in order to understand the conduction mechanism in $GdAlO_3$compound. Thus, the overlapping large polaron tunneling (OLPT) model was the suitable model to explain the mechanism of charge transport in the present ceramic compound.

Acknowledgements

Saji S K aknowledge University Grants Commission (UGC), India for the award of teacher fellowship under the faculty development programme. We are thankful to Dr.Mukul Gupta of UGC-DAE-CSR, Indore for XRD data. we also thank Dr. Archana Lakhani and Dr. A M Awasthi of UGC-DAE-CSR, Indore for providing dielectric measurement facility.

References

1. Vasylechko, L., Senyshyn, A. and Bismayer, U., 2009. Perovskite-type aluminates and gallates. *Handbook on the physics and chemistry of rare earths*, *39*, pp.113-295.
2. Cho, S.Y., Kim, I.T. and Hong, K.S., 1999. Microwave dielectric properties and applications of rare-earth aluminates. *Journal of materials research*, *14*(01), pp.114-119.
3. Sebastian, M.T., 2010. *Dielectric materials for wireless communication*. Elsevier.
4. Raju, G. Seeta Rama, et al. "Synthesis, structural and luminescent properties of Pr 3+ activated GdAlO 3 phosphors by solvothermal reaction method." *Current Applied Physics* 11.3 (2011): S292-S295.
5. Michail, C., Kalyvas, N., Valais, I., David, S., Seferis, I., Toutountzis, A., Karabotsos, A., Liaparinos, P., Fountos, G. and Kandarakis, I., 2013. On the response of GdAlO 3: Ce powder scintillators. *Journal of Luminescence*, *144*, pp.45-52.
6. JCPDF File No.460395.
7. Jonscher, A.K., 1999. Dielectric relaxation in solids. *Journal of Physics D: Applied Physics*, *32*(14), p.R57.
8. Megdiche, M., Perrin-Pellegrino, C. and Gargouri, M., 2014. Conduction mechanism study by overlapping large-polaron tunnelling model in SrNiP 2 O 7 ceramic compound. *Journal of Alloys and Compounds*, *584*, pp.209-215.
9. Ondo-Ndong, R., Ferblantier, G., Pascal-Delannoy, F., Boyer, A. and Foucaran, A., 2003. Electrical properties of zinc oxide sputtered thin films. *Microelectronics journal*, *34*(11), pp.1087-1092.(QMT)
10. Nenasheva, E.A., Kanareykin, A.D., Kartenko, N.F., Dedyk, A.I. and Karmanenko, S.F., 2004. Ceramics materials based on (Ba, Sr) TiO3 solid solutions for tunable microwave devices. *Journal of Electroceramics*, *13*(1-3), pp.235-238. (RF)
11. Stern, F. and Weaver, C., 1970. Dispersion of dielectric permittivity due to space-charge polarization. *Journal of Physics C: Solid State Physics*, *3*(8), p.1736.
12. Kohlrausch, R., 1847. Nachtrag uber die elastiche Nachwirkung beim Cocon und Glasladen. *Ann. Phys.(Leipzig)*, *72*(393), p.7.
13. Bergman, R., 2000. General susceptibility functions for relaxations in disordered systems. *Journal of Applied Physics*, *88*(3), pp.1356-1365.